Journal of Oceanology and Limnology
Vol. 39 No. 3, P. 865-879, 2021
https://doi.org/10.1007/s00343-020-0127-1

Spatial variations of bacterial community composition in sediments of the Jiaozhou Bay, China*

Qiqi SUN[1, 2, 3], Jinming SONG[1, 2, 3, 4, **], Xuegang LI[1, 2, 3, 4], Huamao YUAN[1, 2, 3, 4], Jianwei XING[1, 2, 3]

[1] *Key Laboratory of Marine Ecology and Environmental Sciences*, *Institute of Oceanology*, *Chinese Academy of Sciences*, *Qingdao 266071*, *China*

[2] *Laboratory for Marine Ecology and Environmental Science*, *Pilot National Laboratory for Marine Science and Technology* (*Qingdao*), *Qingdao 266071*, *China*

[3] *Center for Ocean Mega-Science*, *Chinese Academy of Sciences*, *Qingdao 266071*, *China*

[4] *University of Chinese Academy of Sciences*, *Beijing 100049*, *China*

Received Jan. 14, 2020; accepted in principle Mar. 16, 2020; accepted for publication May 3, 2020

Abstract Spatial variations of sediment microbes pose a great challenge for the estimation of anthropogenic influence on biogeochemical processes, yet remain very unclear in coastal ecosystems. Surface sediments in 9 stations from the eutrophic Jiaozhou Bay, China, were sampled, DNA was extracted within the sediments, and the 16S rDNA was sequenced with the Illumina Hiseq sequencing. Results reveal considerable heterogeneity of sediment bacteria in the Jiaozhou Bay, of which Proteobacteria and Bacteroidetes accounted for over 75%. Bacterial alpha-diversity indices decreased generally from the outside to the inner part of the bay and from the offshore to the nearshore area. Bacterial community structures of S3, S4, S7, and S8 clustered, those of S5, S13, and S14 grouped together, while those of S6 and S10 were distinct from each other and from those of the other stations. Major class Gammaproteobacteria were more abundant at the stations with mesoeutrophic to eutrophic levels (S4, S5, S8, and S10) and less abundant at oligotrophic stations (S6, S13, and S14), while Deltaproteobacteria had an opposite distribution pattern. Overall, bacterial community composition transitioned from being Xanthomonadales-dominant at S4 and S8 to being unidentifed_Gammaproteobacteria-dominant at S5, S6, S13, and S14, while in other stations there were comparable orders. The biogeochemical processes correspondingly changed from being nitrogen cycling-dominant at S4 and S8 to being sulfur cycling-dominant at S5, S6, S13, and S14. The bacterial distribution patterns were especially affected by the factors (dissolved organic phosphorus, DOP) in the overlying seawater due to the habitat status of P-insufficiency in the bay. Both orders Xanthomonadales and Alteromonadales could serve as bioindicators of anthropogenic pollution to different pollution types. At last, divergent distribution patterns of individual bacterial populations in the bay were revealed, the influential environmental gradients were clarified, and the uncertainty of microbes was reduced, helping to predict environmental functions in coastal areas.

Keyword: Jiaozhou Bay; bacterial community; spatial variation; sediments; overlying water

1 INTRODUCTION

Microbes are the engine that drives global biogeochemical cycling (Azam and Malfatti, 2007). Sediment microbes (especially bacteria) are a key part of marine ecosystems, which play an important role in regulating the transformations of various biogenic elements (Yokokawa and Nagata, 2010; Sun et al., 2011). For a certain ecosystem, sediment bacterial communities are influenced by their overlying seawater habitats (Stieglmeier et al., 2014). As a complex ecosystem connecting terrestrial and marine habitats (Su et al., 2005), coastal regions

* Supported by the Strategic Priority Research Program of the Chinese Academy of Sciences (No. XDA23050501) and the Key Special Projects of Marine Science and Technology Funds of Shandong Province and Pilot National Laboratory for Marine Science and Technology (Qingdao) (No. 2018SDKJ0504-1)
** Corresponding author: jmsong@qdio.ac.cn

(<200 m in depth) are susceptible to more intensive terrestrial inputs and artificial disturbances (Nogales et al., 2011). These ecosystems always harbor microbial communities in certain degree of spatial heterogeneity due to their large gradients in nutrient concentrations and relevant parameters, etc. (Hewson and Fuhrman, 2004). Such heterogeneity of bacterial communities can lead to additional uncertainty in accurately predicting ecosystem responses to environmental changes and providing better ecosystem services (Kieft et al., 2018). In addition, bacterial communities have served as sensitive indicators of eutrophication and contamination in coastal aquatic sediments due to their sensitivity to environmental changes (Aylagas et al., 2017; Simonin et al., 2019). Considering their key role in ecological function and environmental sustainability, further research is needed regarding bacterial communities in coastal ecosystems and major variables shaping their distribution patterns.

At present, spatial variations of microbes in coastal ecosystems and how they indicate the structure and functioning of marine ecosystems have gained growing attention (Fuhrman et al., 2015), yet the research results varied with ecosystems. It has been widely known that bacterial community composition is more complex in coastal areas such as the Bohai Sea than in open seas such as the northern Yellow Sea (Yu et al., 2018). In recent years, obvious spatial variations have been observed successively in the Jiaozhou Bay (JZB) regarding the sediment ammonia-oxidizing Crenarchaeota (Dang et al., 2008), *NirS*-encoding bacterial assemblages (Dang et al., 2009), ammonia-oxidizing Betaproteobacteria (Dang et al., 2010a) and anammox bacterial communities (Dang et al., 2010b), etc. Research on the sediment bacterial community of four stations in the JZB showed that it was the geographic heterogeneity rather than seasons that determined the benthic microbiomes (Liu et al., 2015). The bacterial community in the Yellow Sea exhibited relatively low spatial variations among the four different coastal sites characterized by rocky, sandy, muddy, and artificial harbors, respectively (Wang et al., 2009). In addition, the negligible spatial variation of bacterioplankton community has been also observed in the Chesapeake Bay (Kan et al., 2007). Usually, the heterogeneity of individual bacterial populations is accompanied by their functional roles and their relative influence on biogeochemical cycling (Kieft et al., 2018). Understanding the bacterial community composition and their influencing factors is key to the accurate prediction of the ecosystem responses to environmental changes and thus providing better ecosystem services.

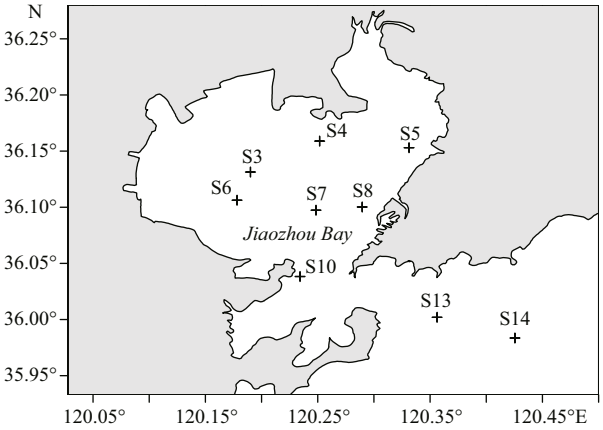

Fig.1 Location of the JZB and sampling stations in November 2019

In this study, bacterial distribution at 9 stations in the JZB was investigated within the surface sediments, with nutrients and relevant parameters determined in the sediments and the overlying seawater. The aims were to present the distribution patterns in bacterial communities of the bay; clarify the influential environmental gradients on the spatial variations of sediment bacterial community composition; and explore possible indicating functions of specific taxa among the bacterial communities.

2 MATERIAL AND METHOD

2.1 Site description and sediment sampling

The JZB (Fig.1) is a large semi-enclosed water body located on the western coast of the Yellow Sea and exchanges with the open sea via a 2.5-km wide mouth (Dai et al., 2007). The mouth of the JZB is narrow and the water-exchange between the inside and the outside of the bay is poor which may constrain the diffusion of the pollutants and the self-purification of the bay. The shallow water column (7 m in average) and JZB tides jointly result in vertical profiles of temperature, turbidity, pH, and dissolved oxygen that were nearly homogeneous. However, the salinity was the greatest at S14 (Table 1). No less than 10 small rivers enter the bay carrying different amounts of sediment and pollutants, especially the Yangge, Dagu, Moshui, Loushan, Licun, and Haibo Rivers (Liu et al., 2011). In recent 30 years, the JZB has experienced various anthropogenic impacts and different eutrophication gradients (Yuan et al., 2016), providing

Table 1 Basic information of individual stations

Station	Longitude (E)	Latitude (N)	Depth (m)	pH	DO (mg/L)	*S*	SPM (mg/L)
S3	120.19°	36.13°	3.9	8.14	12.44	30.96	209.38
S4	120.25°	36.16°	4.7	7.94	10.95	30.89	164.84
S5	120.33°	36.15°	9.0	7.90	11.41	30.77	197.52
S6	120.18°	36.11°	3.5	8.12	13.02	30.93	185.08
S7	120.25°	36.10°	14.2	8.06	11.30	31.97	155.75
S8	120.29°	36.10°	6.2	8.08	12.45	31.00	195.04
S10	120.23°	36.04°	4.6	8.02	10.66	31.03	153.21
S13	120.36°	36.00°	26.0	8.05	10.61	31.03	174.07
S14	120.43°	35.98°	16.3	8.05	10.85	31.99	152.99

DO: dissolved oxygen concentration; *S*: salinity; SPM: suspended material.

an ideal model system for the study of the distribution pattern of coastal microorganisms and related ecological variables.

The field observation was carried out in the JZB cruise onboard the R/V *Chuangxin* (innovation in Chinese) on November 18–19, 2018. During the cruise, 9 stations were deployed over the entire bay and sampled (Fig.1): stations S3, S4, S5, S6, S7, and S8 are located inside the bay, S10 is at the bay mouth, and S13 and S14 are located outside the bay. Basic information of the sampling stations is shown in Table 1. The 9 stations were grouped according to the pollution degree: S4, S5, and S10 are heavily polluted, S3, S6, S7, and S8 are less polluted, and S13 and S14 are affected by seaport and mildly polluted (Liu et al., 2015). It is noteworthy that S10 is the most seriously oil-contaminated station due to the frequent oil-spill events (Dang et al., 2010a) and an anticlockwise eddy, resulting in water quality worsening (Dang et al., 2009). Surficial sediments were sampled using a Van Veen grab sampler and then transported to the laboratory. All sediment samples were deep-frozen immediately after being transferred into the laboratory in 72 h, lyophilized and then ground for chemical analysis.

Seawater at 2 m above the bottom was sampled with 10-L Niskin bottles at each station and analyzed for nutrients and chlorophyll *a* (Chl *a*) (Yuan et al., 2018). After collection, seawater samples were filtered through 47-mm Whatman GF/F filters that were pre-combusted at 450 °C for 4 h and washed (1-mol/L HCl). The filtrates were stored in acid-cleaned HDPE bottles at -20 °C and then brought to the laboratory for dissolved nutrient analysis. The filters were rinsed with distilled water to remove dissolved nutrients after filtration, and then frozen at -20 °C for particulate nutrients analysis. About 200-mL seawater was filtered through 0.45-μm pore-size acetate cellulose filter under low vacuum and then preserved at -20 °C for the Chl *a* analysis. The pH, salinity (*S*), and dissolved oxygen (DO) of the overlying water were measured using a Multi-function Measuring Instrument (Orion, Versa Star, Thermo Fisher Inc., USA) (Budhavant et al., 2014).

2.2 Nutrient determination

Inorganic nitrogen (IN) was extracted in 25-mL 0.1-mol/L HCl for 2 h, with the residue from IN extraction being treated with alkaline $K_2S_2O_8$ at 124 °C for 1 h to digest organic nitrogen (ON) (Liu et al., 2002). Ammonia (NH_4-N), nitrate (NO_3-N) and nitrite (NO_2-N) in the HCl and $K_2S_2O_8$ extracts were then determined photo-metrically following the standard procedure using a continuous flow analyzer (QuAAtro, Bran-Luebbe Inc., Germany) (Xing et al., 2017), the sum of them was IN. Total phosphorus (TP) and inorganic phosphorus (IP) were determined based on HCl-extractable P (1-mol/L HCl, 24 h) of combusted (550 °C, 2 h) and non-combusted sediments, respectively (Aspila et al., 1976), while organic phosphorus (OP) was the difference of TP and IP. A strong alkaline leaching method was adopted for the determination of the biogenic silica (BSi) (Mortlock and Froelich, 1989) and the concentrations of BSi were then converted to weight per mille SiO_2 of dry bulk sediments with the slope for mineral correction (DeMaster, 1981, 1991). The detection limits for NH_4-N, NO_3-N, NO_2-N, dissolved inorganic phosphorus (PO_4-P) and dissolved inorganic silicate (SiO_3-Si) were 0.25, 0.40, 0.01, 0.03, and 0.01 μmol/L, respectively. National standard references were used to satisfy the precision and accuracy. The precisions and recoveries for all nutrient species were better than 5% and between 95.0% and 105.1%, respectively.

Table 2 Nutrient contents in the surface sediments of the JZB

Station	$PINO_3$-N (μg/g)	$PINH_4$-N (μg/g)	PIN (μg/g)	PON (μg/g)	PIP (μg/g)	POP (μg/g)	BSi (g/g)	Chl *a* (μg/g)
S3	3.85	7.20	11.05	74.46	56.45	33.75	0.42	0.42
S4	5.42	7.09	12.51	62.44	96.75	133.70	0.54	0.50
S5	4.13	5.77	9.89	84.12	93.13	203.02	0.64	0.98
S6	5.45	3.70	9.15	15.17	81.26	123.28	0.43	0.32
S7	6.68	14.43	21.10	290.31	113.74	148.70	0.58	0.43
S8	4.66	8.72	13.38	181.50	107.67	127.55	0.55	0.23
S10	3.91	8.56	12.47	97.37	98.69	99.52	0.35	0.19
S13	4.84	13.17	18.01	86.64	104.38	168.18	0.46	0.43
S14	3.80	8.56	12.36	71.49	79.29	86.14	0.44	0.15

$PINO_3$-N and $PINH_4$-N: particle nitrate and ammonia nitrogen in the sediments; PIN and PON: particle inorganic and organic nitrogen; PIP and POP: particle inorganic and organic phosphorus in the sediments; BSi: biogenic silica, mainly SiO_2; Chl *a*: chlorophyll *a*.

Chl *a* on the cellulose-acetate membranes was extracted with 10-mL N, N-dimethylformamide at 4 °C in darkness for 0.5 h and then determined using a fluorescence spectrophotometer (Hitachi F-4600), with the variation coefficient<5% (Suzuki and Ishimaru, 1990).

2.3 DNA extraction and Illumina HiSeq high-throughput sequencing

Total genomic DNA of all sediment examples was extracted using the CTAB/SDS method with Qiagen Gel Extraction Kit (Qiagen, Germany) following the manufacturer's recommendations, with the hypervariable V4 region of the 16S rRNA gene amplified from the bacteria (Caporaso et al., 2011). Sequencing libraries were generated using TruSeq® DNA PCR-Free Sample Preparation Kit (Illumina, USA) and library quality was tested in the Qubit® 2.0 Fluorometer (Thermo Scientific) and Agilent Bioanalyzer 2100 system. Sequencing was conducted on an Illumina HiSeq 2500 platform (Illumina Corporation, San Diego, USA). Approximately 80 117 high-quality prokaryotic sequences per sample with the average length of approximately 420 bp were produced.

2.4 Data analysis

UPARSE software package with the UPARSE-OTU and UPARSE-OTUref algorithms was used in sequence analysis and operational taxonomic units (OTUs) clustering (Edgar, 2013). Taxonomy was assigned using the Ribosomal Database Project classifier (Wang et al., 2007). Each sample was rarefied to the same number of reads (80 117 sequences) for both alpha-diversity and beta-diversity analysis.

Principal Coordinate Analysis (PCoA) was conducted to test the similarity of bacterial community structure of the samples. Pearson correlation analysis was carried out to test the correlations between bacterial communities and influential parameters. Redundancy analysis (RDA) was performed to further identify the influential variable gradients of bacterial groups. Pearson correlation analysis was performed using SPSS 20.0 software (SPSS Inc., Chicago, USA), with $P<0.05$ (two-tailed) being set as the significant level. Analyses of PCoA and RDA were performed with the R software package V.3.6.1 (vegan, ape, ggplot). Surfer 15.0 was used to draw the sampling location map and isolines of bacterial classes in the JZB, with the "Kriging" interpolation method selected. The cumulative histogram was generated using Sigmaplot 12.5 software (Systat Software Inc., San Jose, CA, USA).

3 RESULT

3.1 Nutrients in the sediments and in the overlying water

For most stations, particle organic nitrogen (PON) and particle organic phosphorus (POP) were the main components of total nitrogen (TN) and total phosphorus (TP) in the sediments, while particle inorganic nitrogen (PIN) was characterized by particle ammonia nitrogen ($PINH_4$-N) (Table 2). The nutrient contents in the sampled sediments of the JZB varied with stations. Nutrients such as the particle nitrate nitrogen ($PINO_3$-N), $PINH_4$-N, PIN, PON, and particle inorganic phosphorus (PIP) in the sediments were the greatest at S7 (at the center of the inner bay), while POP, BSi, and Chl *a* had the maximum value at S5 (near the Licun River). The least values of

Table 3 Nutrient concentrations in the overlying seawater of the JZB

Station	NO_3-N (μmol/L)	NH_4-N (μmol/L)	DIN (μmol/L)	DON (μmol/L)	PO_4-P (μmol/L)	DOP (μmol/L)	SiO_3-Si (μmol/L)	Chl *a* (μg/L)
S3	13.75	3.58	19.25	9.25	0.24	2.20	4.44	1.84
S4	19.20	4.38	26.69	4.86	0.47	1.70	6.25	5.40
S5	36.31	8.60	48.90	9.80	1.73	1.23	9.26	2.08
S6	18.53	3.55	23.10	2.00	0.24	0.96	5.03	14.40
S7	9.39	2.09	12.90	13.57	0.20	1.37	3.67	11.72
S8	9.57	1.73	13.19	2.61	0.34	1.45	4.45	6.85
S10	9.74	2.12	13.17	4.34	0.21	0.83	5.05	1.89
S13	9.30	2.79	13.41	0.00	0.21	0.50	4.24	2.17
S14	6.01	1.83	9.38	14.75	0.19	1.11	4.79	2.67

DO: dissolved oxygen concentration; NO_3-N, NH_4-N, and DIN: nitrate, ammonia and dissolved inorganic nitrogen; DON: dissolved organic nitrogen; PO_4-P: dissolved inorganic phosphorus; DOP: dissolved organic phosphorus; SiO_3-Si: dissolved inorganic silicate; Chl *a*: chlorophyll *a*.

$PINH_4$-N, PIN, and PON was recorded at S6 (in the west part of the inner bay), while PIP and POP at S3 (near S6) had the least values. BSi was the least at S10 (at the mouth) and Chl *a* was the least at S14 (outside the bay) (Table 2). BSi showed a positive correlation with Chl *a* (Supplementary Table S1), indicating their common phytoplankton origins.

NO_3-N (in average of 14.64 μmol/L) was the major form of dissolved inorganic nitrogen (DIN), followed by NH_4-N (average of 3.41 μmol/L) (Table 3), which is in line with the findings of a previous study showing that the DIN composition of the JZB has changed from being NH_4-N predominant to NO_3-N predominant due to human intervention in recent years (Li et al., 2018). The overlying seawater of the sampling stations in the JZB also varied in trophic levels. S5 harbored the greatest NO_3-N, NH_4-N, DIN, PO_4-P, and SiO_3-Si, while S14 and S3 had the greatest dissolved organic nitrogen (DON) and dissolved organic phosphorus (DOP), respectively. S13 (outside the bay and near the mouth) had the least DON (0.00 μmol/L) and DOP (0.50 μmol/L), while S14 (outside the bay and away from the mouth) had the least DIN (9.38 μmol/L) and PO_4-P (0.19 μmol/L). S7 had the least SiO_3-Si and the greatest Chl *a* in the overlying water (Table 3), which corresponded well with the greatest *S* (Table 1). Correlation results showed that DIN, PO_4-P, and SiO_3-Si were correlated positively with each other (Supplementary Table S2), which indicated common origins and similar cycling processes (Yuan et al., 2018). Chl *a* in the overlying water showed no correlation with dissolved nutrients. However, Chl *a* in the sediment was significantly and positively correlated with DIN, PO_4-P, and SiO_3-Si (data not shown), which plausibly suggested the relevance of phytoplankton photosynthesis to the inorganic nutrient contents. The DIN/dissolved inorganic phosphorus (DIP) (ranging from 28.2 to 96.3) was greater than the Redfield ratio (16∶1), indicating that the dissolved inorganic matter was more depleted in P than in N (Dortch and Whitledge, 1992; Justić et al., 1995), which was consistent with the general DIP deficiency phenomenon compared with N in the JZB (Yuan et al., 2018).

3.2 Bacterial communities in sediment samples

There were in total 721 055 high-quality sequences for bacterial 16S genes of all sediment samples with an average of 80 117 sequences per sample. Eventually, the bacterial community had 59 929 clustered OTUs. In this study, the rarefaction curves of all the samples tended to be gentle (Fig.2a) with the coverage reaching up to over 99% (Table 4), which indicated that most species had been detected and the dataset could be used in the subsequent analysis. Both Chao1 richness and Shannon diversity indices varied with stations. Most stations had comparable Chao1 richness except stations S3, S7, S13, and S14 which had high values, and most stations had comparable Shannon diversity except stations S4, S8, and S7 which had low values. At most stations, Chao1 richness and Shannon diversity indices had consistent distribution patterns in the JZB, such as at stations S4 and S8 both values of which were lower and at stations S3, S13, and S14 both values of which were higher. Exceptionally, at S7 Chao1 richness was relative higher but Shannon diversity was lower (Table 4), which was plausibly related to its high biomass but high salinity. In contrast, at S5, S6, and S10 relatively lower Chao1 richness but relatively higher Shannon diversity was recorded. PCoA results show that 55.12% and 21.71% of the spatial variations of

Table 4 Diversity indices at 97% sequence similarity of 16S rRNA genes calculated based on 80 117 sequences per sample of bacterial communities

Station	OTU_numbers	Total reads	Coverage (%)	Chao1	ACE	Shannon	Simpson
S3	3 071	80 158	99.2	2 995.0	3 026.9	8.617	0.986
S4	2 571	80 135	99.2	2 582.3	2 604.2	6.073	0.830
S5	2 762	80 116	99.3	2 678.5	2 720.6	8.508	0.991
S6	2 628	80 182	99.3	2 571.5	2 620.3	8.452	0.992
S7	3 090	80 195	99.1	3 043.5	3 077.1	8.062	0.970
S8	2 605	80 099	99.2	2 574.9	2 618.3	7.327	0.941
S10	2 716	80 089	99.4	2 680.3	2 673.4	8.562	0.986
S13	3 358	80 075	99.0	3 364.1	3 392.2	8.912	0.993
S14	3 047	80 006	99.2	2 987.1	3 024.0	8.868	0.993

Chao1 and ACE: Chao1 and ACE richness indices; Shannon and Simpson: the Shannon diversity indices.

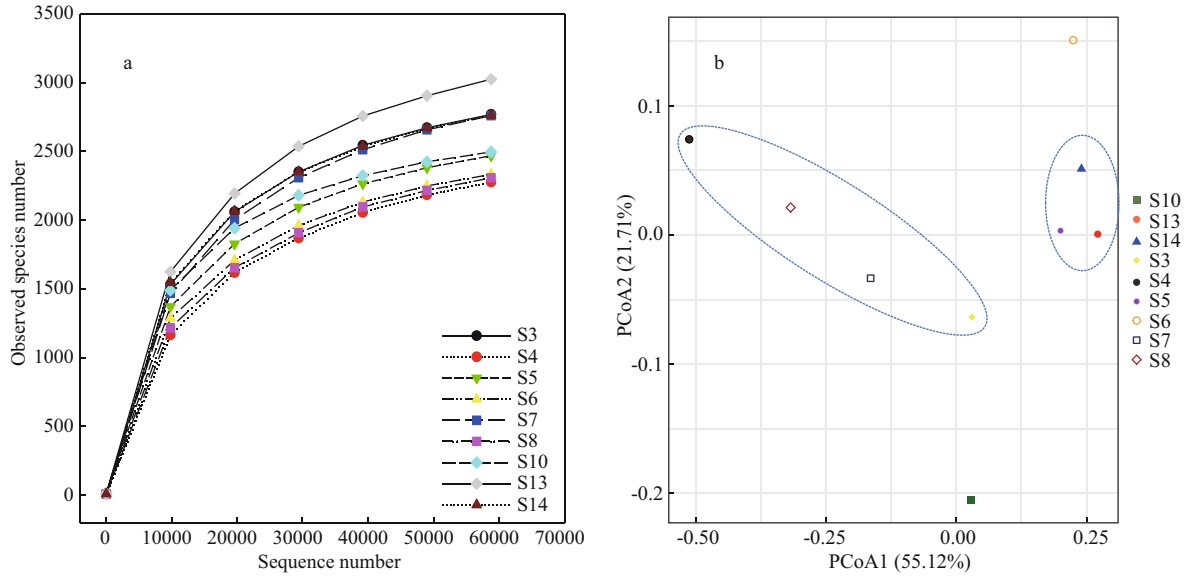

Fig.2 The rarefaction curves based on the observed species (a) and PCoA of bacterial communities in the JZB (b)

bacterial communities could be explained by the first and second axes (P<0.05), indicating a heterogeneous distribution of the bacteria in the sediments of the JZB. DOP was the most important factor loaded on the first axis, while NO_3-N, NH_4-N, DIN, and Chl *a* (in the sediments) were loaded on the second axis. In terms of bacterial community structure, S5, S13, and S14 could be classified as one group, and S3, S4, S7, and S8 could be classified as another group. However, the bacterial community structure of S6 and S10 stood out clearly (Fig.2b).

The bacterial communities across the samples were mainly composed of phyla Proteobacteria, Bacteroidetes, unidentified_Bacteria, Acidobacteria and Chloroflexi, representing 84.1% of the bacterial reads (Fig.3a). At the phylum level, the phyla Proteobacteria (64.9%–83.7%) and Bacteroidetes occupied over 80% at stations S3, S4, S5, S6, and S8, and over 75% at stations S7, S10, S13, and S14. The relative abundances of Proteobacteria and Bacteroidetes were negatively correlated with each other (Supplementary Fig.S1), indicating their opposite trophic strategies. At the class level, Gammaproteobacteria (35.4%–66.3%), Deltaproteobacteria (14.7%–26.8%), Bacteroidia and Alphaproteobacteria occupied over 74% of the total reads (Fig.3b). The relative abundance of Gammaproteobacteria had negative correlations with those of Deltaproteobacteria, Bacteroidia and Alphaproteobacteria in varying degrees (Supplementary Fig.S1). At the order level, Xanthomonadales (1.3%–46.2%), unidentified_Gammaproteobacteria (12.5%–27.3%), Alteromonadales (within Gammaproteobacteria) and Desulfobacterales (4.9%–11.7%, within Deltaproteobacteria) occupied over 30% of the total

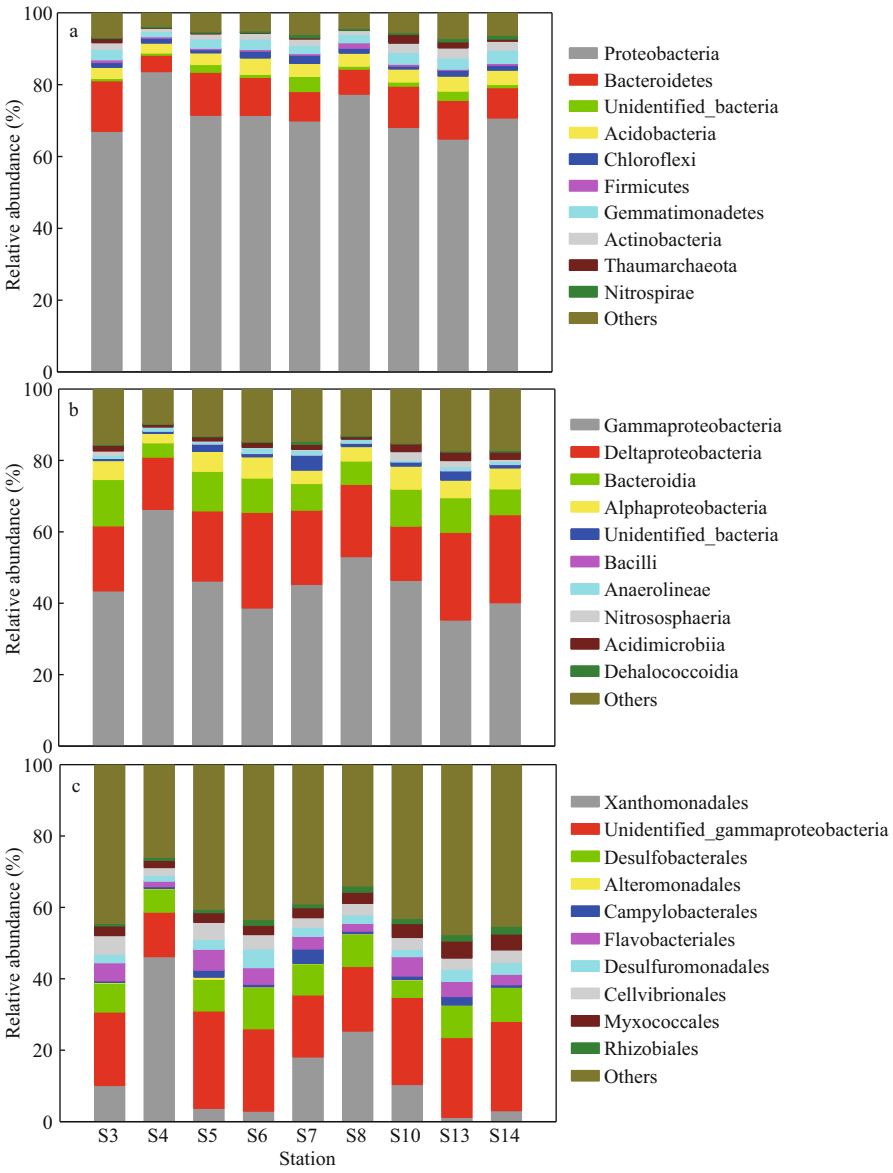

Fig.3 Relative abundances of the bacterial community composition in the sediments of the JZB at the phylum (a), class (b) and order (c) levels

reads (Fig.3c). Negative correlations between the relative abundances of Xanthomonadales and unidentified_Gammaproteobacteria (Supplementary Fig.S1) indicated their opposite trophic strategies.

3.3 Distribution patterns of bacterial communities

Higher levels of Chao1 richness and Shannon diversity indices were generally observed outside the bay such as at stations S13 and S14, and declined from the outer part to the northern part of the bay (Fig.4a & b). The relative abundance of Proteobacteria was found higher at the nearshore stations of the bay (S4: 83.7% and S8: 64.9%) and decreased from the offshore stations in the inner part to the western part of the bay and then to the outside of the bay. However, Proteobacteria tended to be abundant again away from the bay in the open sea (S14). In contrast, high levels of Bacteroidetes were observed in the southwest part of the bay and the mouth, and the levels decreased to the stations outside the bay and then to the nearshore stations S4 and S8.

Similar to that of Proteobacteria, the relative abundance of Gammaproteobacteria was greater at the nearshore stations in the northern part of the bay (S4: 66.3%) and decreased to the mouth (S10: 46.5%), being the least in the western part of the bay (S6: 38.7%) and the outside station (S13: 35.4%), which was found having better water condition in the JZB. Deltaproteobacteria generally presented an opposite pattern to that of Gammaproteobacteria, the

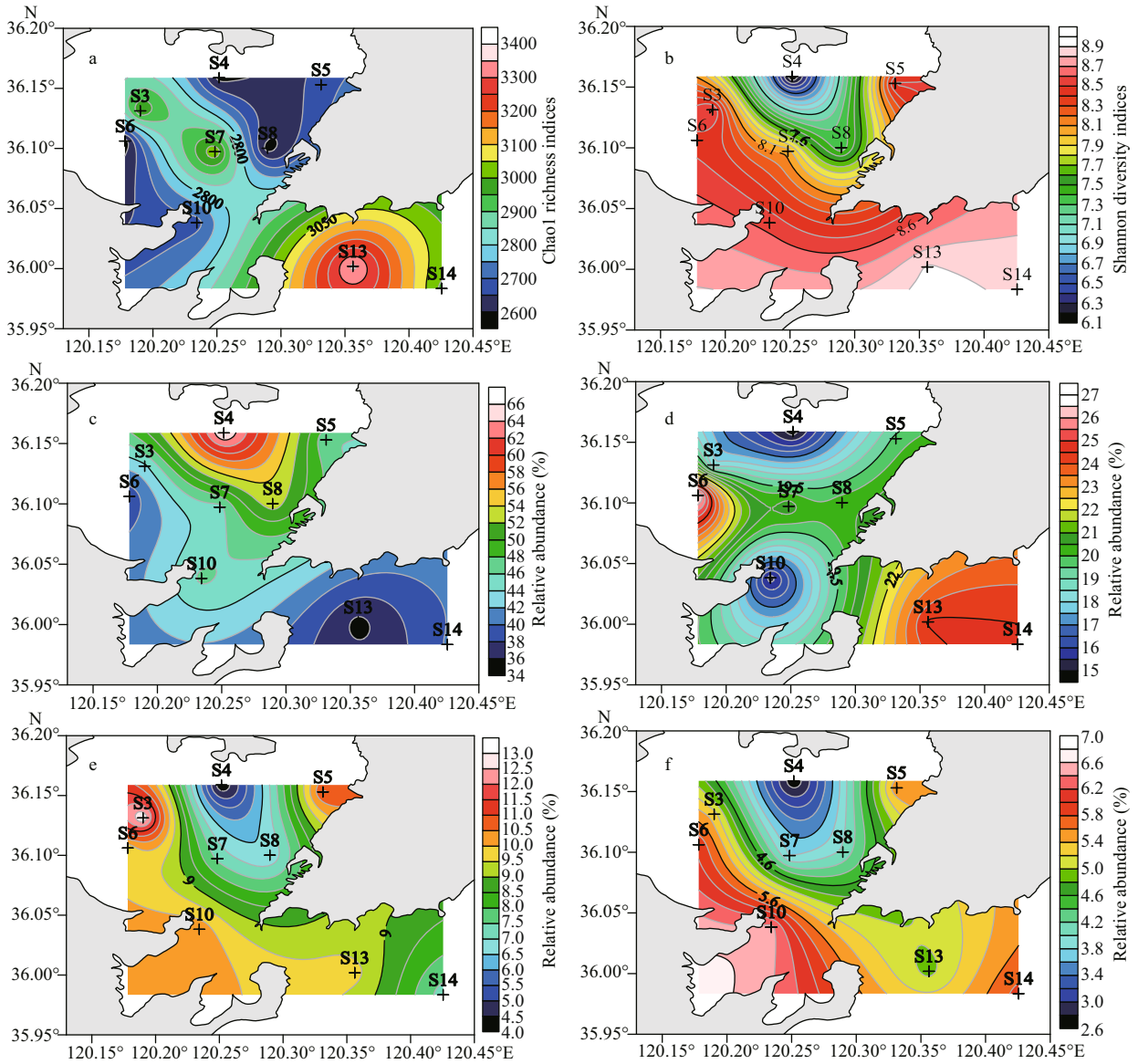

Fig.4 Spatial distributions of species richness (a: Chao1), community diversity (b: Shannon) and predominant classes (c: Gammaproteobacteria; d: Deltaproteobacteria; e: Bacteroidia; f: Alphaproteobacteria) in the sediments of the JZB

abundance of which was higher outside the bay than at the mouth and higher in the western part than in the northern part of the bay. Similar to Bacteroidetes, the relative abundance of Bacteroidia generally increased from the nearshore stations in the northern part of the bay (S4 and S8) to the mouth and then the outer part of the bay, being the greatest in the western and eastern part of the inner bay. Alphaproteobacteria had a similar distribution pattern to that of Bacteroidia. The relative abundance of Alphaproteobacteria generally increased from the northern part of the bay to the outside of the bay and increased from the northern part of the bay to the southwest and northeast of the inner bay (Fig.4).

The relative abundance of Xanthomonadales was similar to that of Gammaproteobacteria, the value of which was the greatest at the nearshore stations (S4 and S8) and decreased from the northern part of the bay to the mouth and then to the outside of the bay. In the bay, Xanthomonadales decreased from the northern part of the bay to the west and east part of the bay. In contrast, the relative abundance of unidentified_Gammaproteobacteria increased from the northern part (S4) of the bay to the outside of the bay, being the greatest at S5. The order Alteromonadales was similar to that of unidentified_ Gammaproteobacteria, being the most abundant at S5. However, the order Desulfobacterales was similar

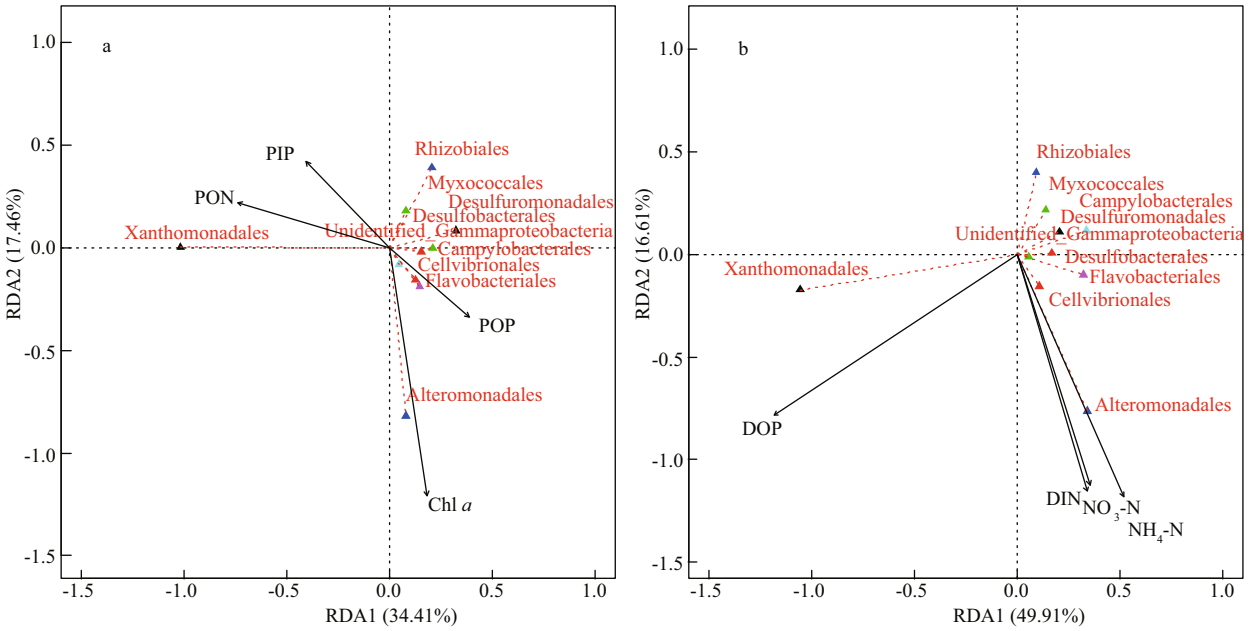

Fig.5 Ordination plots of the results from the redundancy analysis (RDA) to identify relationships between bacterial populations (red dotted arrows) and environmental variables (black solid arrows) in the sediments (a) and in the overlying seawater (b)

to Deltaproteobacteria, being the most abundant at S6 and the least abundant at S10.

3.4 Linking bacterial communities to environmental variables

In the sediments, Chl *a*, PON, PIP, and POP were selected to conduct RDA of the bacteria (Supplementary Table S3; Fig.5a), which could explain 69.4% of the bacterial community composition variation (P<0.05). 34.41% and 17.46% of the spatial variations of bacterial communities among these stations could be explained by the first two axes. However, only Chl *a* (R^2=0.65, P<0.05) was the significant influential factor on the bacterial variation, loaded on the second axis. In the overlying water, DOP, NO_3-N, NH_4-N, and DIN were selected to conduct RDA of the bacteria (Supplementary Table S4; Fig.5b), by which 70.6% of the variation of bacterial community composition could be explained in total (P<0.05). 49.91% and 16.61% of the variations of bacterial communities could be explained by the first two axes. In the overlying water, NH_4-N (R^2=0.69, P<0.05), followed by DOP (R^2=0.63, P<0.1) and then DIN (R^2=0.61, P=0.05) were the main factor gradient influencing the spatial variations of bacterial community composition, with only DOP loaded on the first axis. When the factors in the overlying water and in the sediments were taken together, Chl *a*, NH_4-N, NO_3-N, and DOP were selected to conduct RDA of the bacteria, which could explain 70.6% of the bacterial community composition variation (P<0.05). 37.36% and 15.32% of the total variation of the bacterial communities among these stations were explained by the first two axes. DOP (R^2=0.69, P<0.05), followed by NH_4-N (R^2=0.67, P<0.05) and then NO_3-N (R^2=0.56, P<0.1) were the main factor gradient influencing the spatial variations of bacterial community composition at the sediment-seawater interface (Supplementary Fig.S2).

3.5 Function prediction analysis of sediment bacteria

Function prediction results (Fig.6) show that the OTUs referring to aerobic chemoheterotrophy were higher at S4, S8, S7, and S10 than at S5, S6, S13, and S14, which might reflect the oxygen condition. The OTUs referring to animal parasites and human pathogens were the greatest at S4, followed by S8, S7, and S10, and the least at S13 and S14, which possibly reflected the effects of sewage discharge and anthropogenic pollution. The OTUs referring to nitrate reduction, nitrate respiration and nitrogen respiration indicated a frequently occurring nitrogen metabolism in the sediments, which were significantly greater at S4, S8, S7, S3, and S10 than at S5, S6, S13, and S14. In overall, S5, S6, S13, and S14 were much less affected by the artificial disturbance than S3, S4, S7, S8, and S10, which explained the similar structure

of bacterial communities at S5, S13, and S14.

Correlation analysis results showed that Gammaproteobacteria were positively and Deltaproteobacteria were negatively correlated with all the OTUs referring to human disturbance and nitrogen cycling throughout the profile, which indicated the functional diversity of Proteobacteria. In addition, Deltaproteobacteria were positively correlated with the OTUs referring to respiration of sulfur compounds and sulfate respiration throughout the profile (Supplementary Table S5).

4 DISCUSSION

4.1 Bacterial distribution in the JZB and the influencing factors

The distribution of Chao1 richness and Shannon diversity indices, which generally decreased from the outside to the inner part of the bay and from the offshore to nearshore area (Fig.4), suggested that the bacterial alpha-diversity might be negatively affected by sediment contamination and anthropogenic pollution. The positive correlation between Chao1 richness and PIN H_4-N in the sediments (Supplementary Table S3) suggested that nitrogen deposition might accelerate microbial biomass and bacterial abundance through providing substrate to microbes.

The dominant groups in the sampled sediments differed from those (Proteobacteria, Acidobacteria, Bacteroidetes, Planctomycetes, and Actinobacteria) identified in the previous study at the same site (Liu et al., 2015), which plausibly suggested temporal variations ever since. Gammaproteobacteria and Deltaproteobacteria were the most abundant (Fig.3, >60%), which were consistent with typical marine sediment environment (Liu et al., 2015, 2019). Gammaproteobacteria, the most important group in marine sediments (Yu et al., 2018), were less abundant at the oligotrophic stations S6, S13 and S14, but more abundant at S4, S5, S8, and S10 with high trophic level (Fig.4), indicating their copiotrophic nature (Chigineva et al., 2009; Wang et al., 2012). Gammaproteobacteria were dominated by the aerobic hydrocarbon-degrading Xanthomonadales (Table 4), which was more abundant at S4 (46.2%) and S8 (25.4%), possibly due to their roles in chemoheterotrophy, anthropogenic influence, and nitrogen cycling, while less abundant at S5, S6, S13, and S14 (<10%), due to other processes occurring there (Supplementary Table S5). RDA results showed that the negative effects of DOP were much more than

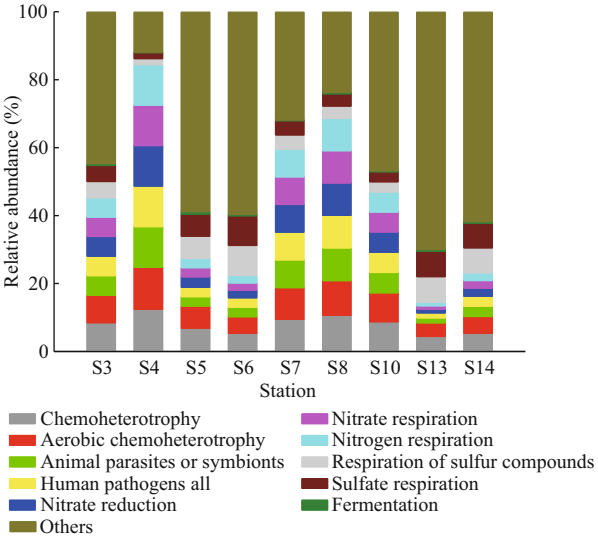

Fig.6 Relative abundances of FAPROTAX function annotation for the bacteria from the sediments in the JZB

the positive effects of NH_4-N and NO_3-N on Xanthomonadales (Fig.5b). Despite lower abundance, the subgroup Alteromonadales was the most active Gammaproteobacteria, indicating its importance in nutrient cycling and overall ecosystem functioning. The positive correlations between the order Alteromonadales and all the dissolved inorganic nutrients (Supplementary Table S4) indicated their copiotrophic nature. In addition, positive correlations of Alteromonadales with Chl *a* both in the sediments (Supplementary Table S3) and in the overlying water (Supplementary Table S4) suggested their relevance in biomass construction, as Alteromonadales was identified as the only group with genes involved in aerobic anoxygenic photosynthesis (Cleary et al., 2017). Therefore, the most abundant Alteromonadales at S5 across stations was the joint results of the greatest nutrients (nitrogen) in the seawater and highest Chl *a* derived from the sediments (Tables 1 & 2). RDA results (Fig.5) show that DOP had positive effects on Alteromonadales such as Chl *a*, NH_4-N, and NO_3-N, and the former might have been transferred into DIP after being utilized by these bacteria. The order Cellvibrionales (within Gammaproteobacteria) was negatively correlated with PIP in the sediments, indicating that PIP was disadvantageous to the survival of this order and sediments with more PIP tended to have less abundant Cellvibrionales and *vice versa*. So far, Cellvibrionales in the JZB or its adjacent Yellow Sea has been seldom reported, despite its role in P cycling. RDA results showed that Chl *a* (in the sediments) had greater effects on bacterial communities than PON, POP, and PIP did in the

sediments (Fig.5a). Overall, DOP had important effects on the most active orders Xanthomonadales and Alteromonadales, and became the most important factor shaping the distribution pattern of sediment bacteria in the JZB (Supplementary Fig.S2). This was consistent with the habitat status of phosphate insufficiency in the bay (Yuan et al., 2018). These results supported the idea that sediment bacteria are profoundly influenced by their habitat in the overlying seawater.

Contrasting distribution patterns of Deltaproteobacteria (i.e., the most abundant at S6, S13, and S14 but the least abundant at S4 and S10, Fig.4) and Gammaproteobacteria indicated the oligotrophic nature of Deltaproteobacteria, which contrasted with the previous report in which Deltaproteobacteria was found abundant in entrophic and anoxic sediments (Bowman and McCuaig, 2003; Liu et al., 2011). The patterns of the predominant members Desulfobacterales and Desulfuromonadales (more abundant at S6, S13, and S14 but less abundant at S4 and S10) were similar to Deltaproteobacteria, as they are chemoorganotrophs related to the degradation of recalcitrant organic matter in global marine sediments (Plugge et al., 2011). It is notable that these predominant orders were in perfect trade-off at S4, where the most abundant Xanthomonadales was accompanied by the least abundant unidentified_ Gammaproteobacteria. Considering the major effects of DOP on Xanthomonadales, we proposed that the riverine inputs at S4 might contain the organic pollutants. The distribution pattern of Alphaproteobacteria was also nearly opposite to that of Gammaproteobacteria, which was less abundant at S4, S7, and S8 but more abundant at S10, S6, and S14 (Fig.4). Alphaproteobacteria was the most abundant at S10 across stations, which suggested that the subgroup was obviously stimulated by the crude oil refining plants and/or played a crucial role in oil-degrading. The predominant order Rhizobiales could play a critical role in carbon and nitrogen cycling of marine ecosystems through photosynthesis. Both orders Myxococcales and Rhizobiales presented a decreasing trend with the increasing TOC in the sampling stations (from S3 to S14) in the overlying water (Supplementary Fig.S1), possibly due to their susceptibility to the more recalcitrant substrates (Cleary et al., 2017). However, such process was depressed by DOP (Supplementary Table S4). The class Bacteroidia was more abundant at the nearshore stations S5 and S10 while less abundant at the nearshore stations S4 and S8 (Fig.3), which might suggest different substrate types from riverine inputs. The predominant order Flavobacteriaceae within Bacteroidia could utilize all kinds of substrates but was extremely enriched with the occurrence of starch (Kieft et al., 2018). Therefore, these bacteria may be enriched because of deposition of the recalcitrant organic matter from the riverine inputs at S5 and S10.

With regard to some rare phyla, unidentified_ Bacteria were the most abundant at S7 across stations (Fig.3) possibly due to PIN and PON being the greatest there (Table 2), which was confirmed by the positive correlations between them (Supplementary Table S3). In this study, unidentified_Bacteria were presumed to be the class Epslionproteobacteria and the predominant order Campylobacterales were reported to be responsible for most denitrification genes in the anaerobic layers of oceans (Llorens-Marès et al., 2015). Therefore, it was considered that S7 (in the deep-water area at the center of the bay) might have anaerobic conditions that were advantageous for the survival and reproduction of these taxa. Similar abundant Campylobacterales at S5 and S13 might also indicate anaerobic conditions. Considering the consistent Chl *a* and *S* in the overlying water, the greatest Campylobacterales at S7 among stations was also related to the unique condition characterized by high salinity and high biomass. As such, phyla Chloroflexi and Nitrospirae that were closely related to Chl *a* also hiked at S7. The distribution of Acidobacteria (more abundant at S6, S13, and S14 but less abundant at S3, S4, and S5) was possibly related to their susceptibility to the more recalcitrant substrates, i.e., oligotrophic nature (Fierer et al., 2007; Zhang et al., 2016). The negative correlation between Acidobacteria and DOP suggested their involvement in P cycling (Supplementary Table S4). In addition, the ubiquitous Acidobacteria in the JZB might also imply acidification.

4.2 Possible bioindicator taxa in the assessment of the anthropogenic pollution

Our results showed that anthropogenic pollution profoundly altered the bacterial community composition among stations, which could be indicated by the order Xanthomonadales (Gammaproteobacteria) (Fig.3c). That was, S4 (near the Hongdao aquiculture area) and S8 (near the Qingdao Port), harbored the most abundant Xanthomonadales due to the most river input and livestock wastes. S7 (located at the center of the bay), S10 (at the mouth), and S3 (at the

northwest) had comparable Xanthomonadales and unidentified_Gammaproteobacteria. However, both S5 (located at the estuary of Licun River) and the less-polluted S6, S13, and S14 held the most abundant unidentified_Gammaproteobacteria. Overall, the bacterial community composition transitioned from being Xanthomonadales-dominant at S4 and S8 to being unidentified_Gammaproteobacteria-dominant at S5, S6, S13, and S14. The predicting function correspondingly changed from being nitrogen cycling-dominant at S4 and S8 to being sulfur cycling-dominant at S5, S6, S13 and S14 (Supplementary Table S5). This could be partly caused by the organic pollutants from livestock and industrial wastes that entered the JZB. The order Xanthomonadales (genus *Stenotrophomonas*) has been used as a bioindicator for the detection of the impact of multiple contamination sources by polycyclic aromatic hydrocarbons (PAHs) on the bacterial community (Juhasz et al., 2000; Kanaly and Harayama, 2010). Strains of the genus *Stenotrophomonas* have been reported as PAHs- and Triton X-100- degrading bacteria (Chen et al., 2004; Gutierrez et al., 2013). Therefore, we proposed that the order Xanthomonadales holds the potential of indicating the anthropogenic organic pollution in the JZB. On the other hand, there were positive correlations between Alteromonadales and dissolved inorganic nutrients rather than organic components (Supplementary Table S5), which indicated their sensitivity to the dissolved inorganic nutrients and suggested the potential of this subgroup as a bioindicator of inorganic pollution. As reported, Alteromonadales are mainly aerobic chemoheterotrophic species that decompose the primary produced carbon sources (Naghoni et al., 2017) and accounted significantly for the DIC-assimilating Gammaproteobacteria (DeLorenzo et al., 2012), which might be enhanced by the inorganic nutrients. However, inorganic pollution possibly failed to change the composition of the bacterial communities in the JZB, which is why the bacterial community composition at S5 showed a little difference from those of S13 and S14 in the open sea. In addition, the positive correlation between Deltaproteobacteria and the OTUs referring to the respiration of sulfur compounds and sulfate respiration (Supplementary Table S5) verified the application of Deltaproteobacteria as a sensitive indicator of sulfate-reducing bacteria (SRB) (Ravenschlag et al., 2000; Liu et al., 2015). Deltaproteobacteria could also serve as a negative indicator of anthropogenic pollution in the JZB due to their negative correlation with all the OTUs referring to anthropogenic influences and nitrogen cycling.

In this study, the Pearson correlations between bacterial orders and environmental factors were confirmed by the redundancy analysis, with $P<0.05$ being set as the significant level ($n=9$), while those between bacterial orders and OTUs indicating biogeochemical processes were confirmed by literature, both excluded the causality of correlation results. Our results provided profound evidence supporting the indicating function of bacteria. Nevertheless, given the extreme complexity of microbial communities in marine ecosystems in terms of distribution and functions, our results should be interpreted with great caution regarding the indicating functions of bacteria, which needs further experimental verification and evidence. This study supports the idea that bacterial communities could serve as sensitive indicators of anthropogenic pollution, providing an effective and sensitive tool for rapid environmental assessment (Simonin et al., 2019).

5 CONCLUSION

The bacterial communities in the sediments presented considerable spatial variations across the JZB, with Proteobacteria and Bacteroidetes being the most abundant. More specifically, bacterial alpha-diversity indices decreased from the outside to the inner part of the bay and from the offshore to the nearshore area. Bacterial community structures of S3, S4, S7, and S8 clustered; those of S5, S13, and S14 could also be classified as one group, while those of S6 and S10 were distinct from each other and from the other stations. Overall, the bacterial community composition transitioned from being Xanthomonadales-dominant at S4 and S8 to being unidentified_Gammaproteobacteria-dominant at S5, S6, S13, and S14, while in other stations they had comparable values. Among stations, Gammaproteobacteria (order Xanthomonadales) were more abundant at the nearshore stations (S4 and S8) which receive the most freshwater inputs and suffer from the livestock wastes but were less abundant in stations having better environmental conditions (S5, S6, S13, and S14). The distribution, together with their positive correlations with the OTUs referring to human activities and nitrogen cycling, indicated the potential of Xanthomonadales as a sensitive indicator for sediment contamination

and/or anthropogenic pollution. Deltaprotepbacteria presented opposite distribution patterns with Gammaproteobacteria, suggesting their contrasting trophic strategies (oligotrophic vs. copiotrophic). The bacterial distribution was affected by especially the factors (DOP) in the overlying seawater, possibly related to the habitat status of a general P insufficiency in the bay.

Since microbes responding to the overweight inputs of nutrients are indicative for the estimation of anthropogenic influence on the biogeochemical processes, this work is of great importance for understanding coastal ecosystems and human influence on them. Our results identified the relevance of bacterial information in nutrient cycling as well their indicating functions to sediment contamination and/or anthropogenic pollution. Bacterial indicators could complement the information regarding human-induced impacts, which however has not been well researched. Further investigation of specific bacterial taxa responding to selected pollutants may help to improve our understanding of the indicating functions of bacterial communities.

6 DATA AVAILABILITY STATEMENT

The datasets generated during the current study are available from the corresponding author on reasonable request.

7 ACKNOWLEDGMENT

The authors thank the crews of R/V *Chuangxin* for supports in data collection, and Prof. SUN Xiaoxia for support in Chl *a* data processing.

References

Aspila K I, Agemian H, Chau A S Y. 1976. A semi-automated method for the determination of inorganic, organic and total phosphate in sediments. *Analyst*, **101**(1200): 187-197.

Aylagas E, Borja Á, Tangherlini M, Dell'Anno A, Corinaldesi C, Michell C T, Irigoien X, Danovaro R, Rodríguez-Ezpeleta N. 2017. A bacterial community-based index to assess the ecological status of estuarine and coastal environments. *Marine Pollution Bulletin*, **114**(2): 679-688.

Azam F, Malfatti F. 2007. Microbial structuring of marine ecosystems. *Nature Reviews Microbiology*, **5**(10): 782-791.

Bowman J P, McCuaig R D. 2003. Biodiversity, community structural shifts, and biogeography of prokaryotes within Antarctic continental shelf sediment. *Applied and Environmental Microbiology*, **69**(5): 2 463-2 483.

Budhavant K B, Rao P S P, Safai P D, Granat L, Rodhe H. 2014. Chemical composition of the inorganic fraction of cloud-water at a high altitude station in West India. *Atmospheric Environment*, **88**: 59-65.

Caporaso J G, Lauber C L, Walters W A, Berg-Lyons D, Lozupone C A, Turnbaugh P J, Fierer N, Knight R. 2011. Global patterns of 16s rRNA diversity at a depth of millions of sequences per sample. *Proceedings of the National Academy of Sciences of the United States of America*, **108**(S1): 4 516-4 522.

Chen H J, Huang S L, Tseng D H. 2004. Aerobic biotransformation of octylphenol polyethoxylate surfactant in soil microcosms. *Environmental Technology*, **25**(2): 201-210.

Chigineva N I, Aleksandrova A V, Tiunov A V. 2009. The addition of labile carbon alters litter fungal communities and decreases litter decomposition rates. *Applied Soil Ecology*, **42**(3): 264-270.

Cleary D F R, Coelho F J R C, Oliveira V, Gomes N C M, Polónia A R M. 2017. Sediment depth and habitat as predictors of the diversity and composition of sediment bacterial communities in an inter-tidal estuarine environment. *Marine Ecology*, **38**(2): e12411.

Dai J C, Song J M, Li X G, Yuan H M, Li N, Zheng G X. 2007. Environmental changes reflected by sedimentary geochemistry in recent hundred years of Jiaozhou Bay, North China. *Environmental Pollution*, **145**(3): 656-667.

Dang H Y, Chen R P, Wang L, Guo L Z, Chen P P, Tang Z W, Tian F, Li S Z, Klotz M G. 2010a. Environmental factors shape sediment anammox bacterial communities in hypernutrified Jiaozhou Bay, China. *Applied and Environmental Microbiology*, **76**(21): 7 036-7 047.

Dang H Y, Li J, Chen R P, Wang L, Guo L Z, Zhang Z N, Klotz M G. 2010b. Diversity, abundance, and spatial distribution of sediment ammonia-oxidizing *Betaproteobacteria* in response to environmental gradients and coastal eutrophication in Jiaozhou Bay, China. *Applied and Environmental Microbiology*, **76**(14): 4 691-4 702.

Dang H Y, Wang C Y, Li J, Li T G, Tian F, Jin W, Ding Y S, Zhang Z N. 2009. Diversity and distribution of sediment *NirS*-encoding bacterial assemblages in response to environmental gradients in the Eutrophied Jiaozhou Bay, China. *Microbial Ecology*, **58**(1): 161-169.

Dang H Y, Zhang X X, Sun J, Li T G, Zhang Z N, Yang G P. 2008. Diversity and spatial distribution of sediment ammonia-oxidizing crenarchaeota in response to estuarine and environmental gradients in the Changjiang estuary and East China Sea. *Microbiology*, **154**(7): 2 084-2 095.

DeLorenzo S, Bräuer S L, Edgmont C A, Herfort L, Tebo B M, Zuber P. 2012. Ubiquitous dissolved inorganic carbon assimilation by marine bacteria in the Pacific Northwest coastal ocean as determined by stable isotope probing. *PLoS One*, **7**(10): e46695.

DeMaster D J. 1981. The supply and accumulation of silica in the marine environment. *Geochimica et Cosmochimica Acta*, **45**(10): 1 715-1 732.

DeMaster D J. 1991. Measuring biogenic silica in marine

sediments and suspended matter. *In*: Hurd D C, Spencer D W eds. Marine Particles: Analysis and Characterization. AGU, Washington. p.363-367.

Dortch Q, Whitledge T E. 1992. Does nitrogen or silicon limit phytoplankton production in the Mississippi River plume and nearby regions? *Continental Shelf Research*, **12**(11): 1 293-1 309.

Edgar R C. 2013. UPARSE: highly accurate OTU sequences from microbial amplicon reads. *Nature Methods*, **10**(10): 996-998.

Fierer N, Bradford M A, Jackson R B. 2007. Toward an ecological classification of soil bacteria. *Ecology*, **88**(6): 1 354-1 364.

Fuhrman J A, Cram J A, Needham D M. 2015. Marine microbial community dynamics and their ecological interpretation. *Nature Reviews Microbiology*, **13**(3): 133-146.

Gutierrez T, Green D H, Nichols P D, Whitman W B, Semple K T, Aitken M D. 2013. *Polycyclovorans algicola* gen. nov., sp. nov., an aromatic-hydrocarbon-degrading marine bacterium found associated with laboratory cultures of marine phytoplankton. *Applied and Environmental Microbiology*, **79**(1): 205-214.

Hewson I, Fuhrman J A. 2004. Richness and diversity of bacterioplankton species along an estuarine gradient in Moreton Bay, Australia. *Applied and Environmental Microbiology*, **70**(6): 3 425-3 433.

Juhasz A L, Stanley G A, Britz M L. 2000. Microbial degradation and detoxification of high molecular weight polycyclic aromatic hydrocarbons by *Stenotrophomonas maltophilia* strain VUN 10, 003. *Letters in Applied Microbiology*, **30**(5): 396-401.

Justić D, Rabalais N N, Turner R E. 1995. Stoichiometric nutrient balance and origin of coastal eutrophication. *Marine Pollution Bulletin*, **30**(1): 41-46.

Kan J J, Suzuki M T, Wang K, Evans S E, Chen F. 2007. High temporal but low spatial heterogeneity of bacterioplankton in the Chesapeake Bay. *Applied and Environmental Microbiology*, **73**(21): 6 776-6 789.

Kanaly R A, Harayama S. 2010. Advances in the field of high-molecular-weight polycyclic aromatic hydrocarbon biodegradation by bacteria. *Microbial Biotechnology*, **3**(2): 136-164.

Kieft B, Li Z, Bryson S, Crump B C, Hettich R, Pan C L, Mayali X, Mueller R S. 2018. Microbial community structure-function relationships in Yaquina Bay estuary reveal spatially distinct carbon and nitrogen cycling capacities. *Frontiers in Microbiology*, **9**: 1 282.

Li K Q, He J, Li J L, Guo Q, Liang S K, Li Y B, Wang X L. 2018. Linking water quality with the total pollutant load control management for nitrogen in Jiaozhou Bay, China. *Ecological Indicators*, **85**: 57-66.

Liu J J, Diao Z H, Xu X R, Xie Q. 2019. Effects of dissolved oxygen, salinity, nitrogen and phosphorus on the release of heavy metals from coastal sediments. *Science of the Total Environment*, **666**: 894-901.

Liu S M, Ye X W, Zhang J, Zhao Y F. 2002. Problems with biogenic silica measurement in marginal seas. *Marine Geology*, **192**(4): 383-392.

Liu X, Hu H W, Liu Y R, Xiao K Q, Cheng F S, Li J, Xiao T. 2015. Bacterial composition and spatiotemporal variation in sediments of Jiaozhou Bay, China. *Journal of Soils and Sediments*, **15**(3): 732-744.

Liu X, Xiao T, Luan Q S, Zhang W Y, Wang M Q, Yue H D. 2011. Bacterial diversity, composition and temporal-spatial variation in the sediment of Jiaozhou Bay, China. *Chinese Journal of Oceanology and Limnology*, **29**(3): 576-590.

Llorens-Marès T, Yooseph S, Goll J, Hoffman J, Vila-Costa M, Borrego C M, Dupont C L, Casamayor E O. 2015. Connecting biodiversity and potential functional role in modern euxinic environments by microbial metagenomics. *The ISME Journal*, **9**(7): 1 648-1 661.

Mortlock R A, Froelich P N. 1989. A simple method for the rapid determination of biogenic opal in pelagic marine sediments. *Deep Sea Research Part A. Oceanographic Research Papers*, **36**(9): 1 415-1 426.

Naghoni A, Emtiazi G, Amoozegar M A, Cretoiu M S, Stal L J, Etemadifar Z, Shahzadeh Fazeli S A, Bolhuis H. 2017. Microbial diversity in the hypersaline Lake Meyghan, Iran. *Scientific Reports*, **7**(1): 11 522.

Nogales B, Lanfranconi M P, Piña-Villalonga J M, Bosch R. 2011. Anthropogenic perturbations in marine microbial communities. *FEMS Microbiology Reviews*, **35**(2): 275-298.

Plugge C M, Zhang W W, Scholten J C M, Stams A J M. 2011. Metabolic flexibility of sulfate-reducing bacteria. *Frontiers in Microbiology*, **2**: 81.

Ravenschlag K, Sahm K, Knoblauch C, Jørgensen B B, Amann R. 2000. Community structure, cellular rRNA content, and activity of sulfate-reducing bacteria in marine arctic sediments. *Applied and Environmental Microbiology*, **66**(8): 3 592-3 602.

Simonin M, Voss K A, Hassett B A, Rocca J D, Wang S Y, Bier R L, Violin C R, Wright J P, Bernhardt E S. 2019. In search of microbial indicator taxa: shifts in stream bacterial communities along an urbanization gradient. *Environmental Microbiology*, **21**(10): 3 653-3 668.

Stieglmeier M, Klingl A, Alves R J E, Rittmann S K M R, Michael M, Leisch N, Schleper C. 2014. *Nitrososphaera viennensis* gen. nov., sp. nov., an aerobic and mesophilic, ammonia-oxidizing archaeon from soil and a member of the archaeal phylum *Thaumarchaeota*. *International Journal of Systematic and Evolutionary Microbiology*, **64**(8): 2 738-2 752.

Su M L, Jing Z, Hong T C, Guo S Z. 2005. Factors influencing nutrient dynamics in the eutrophic Jiaozhou Bay, North China. *Progress in Oceanography*, **66**(1): 66-85.

Sun F L, Wang Y S, Wu M L, Wang Y T, Li Q P. 2011. Spatial heterogeneity of bacterial community structure in the sediments of the Pearl River estuary. *Biologia*, **66**(4): 574-584.

Suzuki R, Ishimaru T. 1990. An improved method for the determination of phytoplankton chlorophyll using N, N-dimethylformamide. *Journal of the Oceanographical*

Society of Japan, **46**(4): 190-194.

Wang H Y, Jiang X L, He Y, Guan H S. 2009. Spatial and seasonal variations in bacterial communities of the Yellow Sea by T-RFLP analysis. *Frontiers of Environmental Science & Engineering in China*, **3**(2): 194-199.

Wang H, He Z L, Lu Z M, Zhou J Z, Van Nostrand J D, Xu X H, Zhang Z J. 2012. Genetic linkage of soil carbon pools and microbial functions in subtropical freshwater wetlands in response to experimental warming. *Applied and Environmental Microbiology*, **78**(21): 7 652-7 661.

Wang Q, Garrity G M, Tiedje J M, Cole J R. 2007. Naïve bayesian classifier for rapid assignment of rRNA sequences into the new bacterial taxonomy. *Applied and Environmental Microbiology*, **73**(16): 5 261-5 267.

Xing J W, Song J M, Yuan H M, Li X G, Li N, Duan L Q, Kang X M, Wang Q D. 2017. Fluxes, seasonal patterns and sources of various nutrient species (nitrogen, phosphorus and silicon) in atmospheric wet deposition and their ecological effects on Jiaozhou Bay, North China. *Science of the Total Environment*, **576**: 617-627.

Yokokawa T, Nagata T. 2010. Linking bacterial community structure to carbon fluxes in marine environments. *Journal of Oceanography*, **66**(1): 1-12.

Yu S X, Pang Y L, Wang Y C, Li J L, Qin S. 2018. Distribution of bacterial communities along the spatial and environmental gradients from Bohai Sea to northern Yellow Sea. *PeerJ*, **6**: e4272.

Yuan H M, Song J M, Xing J W, Li X G, Li N, Duan L Q, Qu B X, Wang Y D. 2018. Spatial and seasonal variations, partitioning and fluxes of dissolved and particulate nutrients in Jiaozhou Bay. *Continental Shelf Research*, **171**: 140-149.

Yuan Y, Song D H, Wu W, Liang S K, Wang Y, Ren Z P. 2016. The impact of anthropogenic activities on marine environment in Jiaozhou Bay, Qingdao, China: a review and a case study. *Regional Studies in Marine Science*, **8**: 287-296.

Zhang C, Liu G B, Xue S, Wang G L. 2016. Soil bacterial community dynamics reflect changes in plant community and soil properties during the secondary succession of abandoned farmland in the Loess Plateau. *Soil Biology and Biochemistry*, **97**: 40-49.

Electronic supplementary material

Supplementary material (Supplementary Tables S1–S5 and Figs.S1–S2) is available in the online version of this article at https://doi.org/10.1007/s00343-020-0127-1.